Tellus (1992), *44B*, 409–421

An analysis of 5-day midtropospheric flow patterns for the South Pole: 1985–1989

By JOYCE M. HARRIS, *Climate Monitoring and Diagnostics Laboratory, National Oceanic and Atmospheric Administration, 325 Broadway, Boulder, Colorado 80303, USA*

(Manuscript received 12 November 1991; in final form 21 April 1992)

ABSTRACT

An analysis of 5-day midtropospheric flow patterns for the South Pole during 1985–1989 is presented. Cluster analysis was used to summarize trajectories by year and by month. The results indicate that flow from the east was most often anticyclonic and light, occurring 8–18% of the time. Westerly flow patterns were the strongest and most frequent (37–51% occurrence). They were consistently cyclonic, usually reflecting storms in the Ross Sea area, the average center of the circumpolar vortex. Strong northerly flow occurred more often in 1987 than in other years. Year-to-year variability was also evident in southwesterly flow, which was enhanced in 1988, and weaker in 1987, compared with other years. The lightest winds over the South Pole occur during January, while the most vigorous long-range transport to South Pole occurs from July through October. Selected isentropic trajectories were examined to determine errors inherent in the isobaric estimates. Isentropic trajectories from the east showed little vertical motion and good agreement with isobaric ones. Over west Antarctica, however, isentropic trajectories consistently showed positive vertical motion. As a result, their isobaric counterparts were too long and overestimated the cyclonic curvature in the flow. Preferred transport from the west with warm-air advection results from the circumpolar vortex being asymmetrical, and the average isotherms, though roughly circular, being offset to the east of the South Pole.

1. Introduction

The South Pole has few rivals when it comes to barren, pristine sites far removed from civilization or an abundance of other life. Its location deep within the Antarctic continent (Fig. 1), the gentle slope of its snow-covered surroundings, and the absence of a diurnal solar cycle make the South Pole a unique and rewarding place to study the dynamics and chemistry of earth's atmosphere. NOAA's Climate Monitoring and Diagnostics Laboratory, in cooperation with the National Science Foundation, measures ozone and other trace gases, aerosols, solar radiation, and meteorology at Amundsen-Scott South Pole Observatory (SPO). These efforts are geared toward understanding background conditions of the atmosphere and how they are being modified by human activities.

The purpose of this paper is to describe common midtropospheric flow patterns for SPO based on 5 years (1985–1989) of atmospheric trajectories. Cluster analysis, a multivariate statistical technique, is used to group trajectories according to wind speed and direction. This procedure uses a mathematical criterion to ensure similarity among the trajectories in each group or cluster. Each transport cluster can then be described by a mean trajectory or "cluster mean" that best represents all the trajectories in that cluster. In this way, many trajectories can be summarized in a limited space. Trajectories are processed by year and by month to summarize interannual and seasonal changes in the wind regime.

The first studies using cluster analysis with atmospheric trajectories were performed by Moody (1986) and Moody and Galloway (1988). This technique was used by Harris and Kahl (1990) to describe a flow climatology for Mauna Loa Observatory on Hawaii; the technique is documented in detail there. A follow-on of the Harris and Kahl study by Harris *et al.* (1992)

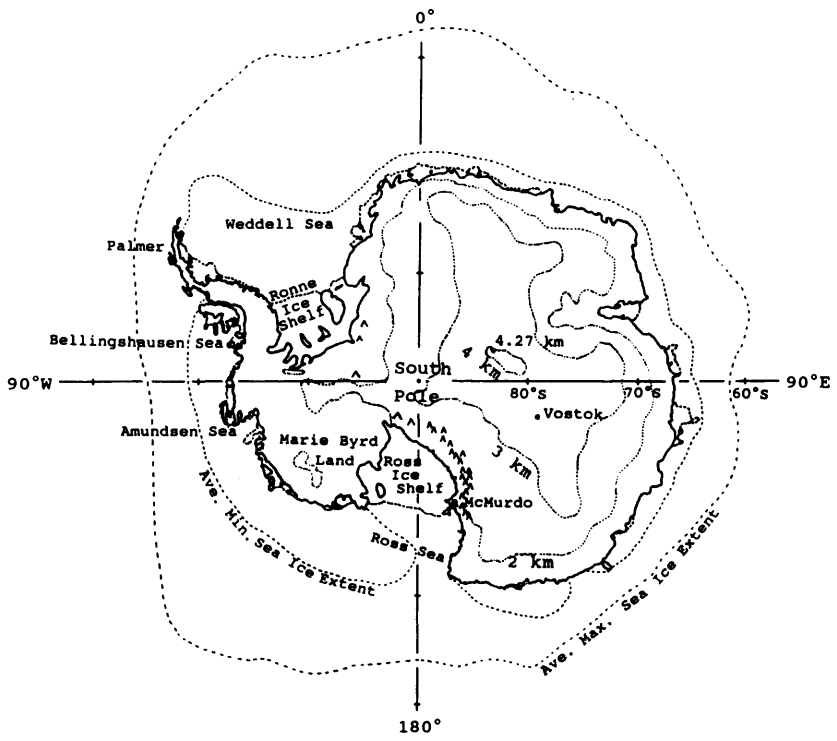

Fig. 1. Map of Antarctica showing height contours and extent of sea ice.

examined Mauna Loa methane measurements according to transport type to determine effects of sources, sinks, and flow patterns on methane variability.

2. Factors determining transport to the South Pole observatory

The chief elements affecting climate at SPO are heat loss through radiation, heat gain through horizontal advection of air from lower latitudes, and prevailing downward motion (Schwerdtfeger, 1970; Stone and Kahl, 1991). SPO at 2.8 km msl sits on the flank of a dome of ice covering most of the continent; that dome attains a maximum depth of 4.27 km to the northeast. (Because every direction with respect to the South Pole is north, we use the convention in this paper of giving compass directions with respect to grid north at 0° longitude; see the map in Fig. 1.) The average surface pressure at SPO is about 680 hPa. Surface winds are determined by strong radiational cooling and the gradually sloping terrain of the polar plateau (Schwerdtfeger, 1984). At SPO these "inversion" winds flow from the northeast sector and are known for their directional constancy. They are usually decoupled from the midtropospheric flow by a strong surface inversion extending to about 600 hPa in summer, and to somewhat lower altitudes in winter (Samson, 1983). The overall subsidence over the continent and katabatic outflow of cold air from the continent are compensated by warm-air advection above the inversion. Thus, Antarctica acts as a heat sink for the Southern Hemisphere having an estimated total advective heat gain of 15×10^{21} cal year^{-1} balanced by heat loss through the top of the atmosphere (Schwerdtfeger, 1970). Long-range transport, aside from being critical to the Antarctic heat budget, also affects the aerosol composition, ozone concentration, moisture content, and clouds in the troposphere above SPO. Sea-salt events in surface aerosols occur when

coastal storms travel inland bringing warm, moist, marine air to the region (Hogan and Barnard, 1978; Parungo *et al.*, 1981; Bodhaine et al., 1986). A weakening of the inversion, due to surface warming and turbulent mixing, allows the aerosol to be detected at the surface.

An increase in transport of ozone-depleted air from lower latitudes may have contributed to the downward trend in the SPO surface ozone concentration during summer (Schnell et al., 1991). Evidence of enhanced transport is provided by a downward trend in solar irradiance corresponding to increased cloudiness during January and February (Dutton et al., 1991). Samson (1983) and Stone and Kahl (1991) have linked periods of winter cloudiness to rapid transport of warm, moist air from the northwest, initiated by strong cyclones in the Weddell Sea area, combined with a ridge of high pressure to the northeast.

The most effective long-range transport to SPO occurs after sunset. Then, the meridional temperature gradient strengthens, resulting in baroclinic instability that is manifested in intense cyclones along the coast. The string of cyclones in the subpolar belt creates a vortex of zonal flow around the Antarctic coast. The circumpolar vortex is neither circular nor centered at the pole. In all likelihood, the asymmetry of the polar vortex results from two deep indentations in the continent corresponding to the Weddell and Ross Seas. The position of the vortex center is frequently near the Ross Ice Shelf (Schwerdtfeger, 1984). The synoptic situation over Antarctica often includes lows over this area, Marie Byrd Land, and/or the Weddell Sea/Ronne Ice Shelf. A semipermanent high is often centered near 80°S, 80°E, over the polar plateau in east Antarctica (Samson, 1983). The exact positions and strengths of these synoptic features determine if and when subpolar air is transported to SPO.

3. Trajectory data base

Isobaric back trajectories on the 500-hPa surface were calculated twice daily at 0000 and 1200 UT for 1985–1989. The 500-hPa level was chosen to represent flow in the midtroposphere above the surface inversion. More than 99% of all possible trajectories for the period were available for the analysis. Only 10 out of a total of 3642 trajectories were missing. Trajectories were calculated 5 days back, a sufficient duration to diagnose rapid transport from open coastal waters.

Isentropic trajectories are usually preferable to isobaric ones, since they account for adiabatic vertical motions along the path of the wind. Unfortunately, for large studies of this type, we must rely primarily on isobaric trajectories because of computer resource limitations. However, selected isentropic trajectories were computed to determine the effects of vertical motions on typical transport paths. These results are included in Section 5.

The trajectory models were documented by Harris (1982) and Harris and Bodhaine (1983). Meteorological data for the current study was provided by the European Centre for Medium Range Weather Forecasts (ECMWF) in the form of global gridded analyses from the World Meteorological Organization archive. These data were produced twice daily on 2.5° grids at seven mandatory pressure surfaces: 1000, 850, 700, 500, 300, 200, and 100 hPa. Trenberth and Olson (1988) recommended this data set over the analysis produced by the National Meteorological Center (NMC) for the Southern Hemisphere, and cited specific problems with the NMC analysis for Antarctica until May 1986. They reported a gradual improvement with time for the ECMWF analyses, though they noted problems communicating the data taken over Antarctica as of 1986.

Much uncertainty in the wind field over Antarctica derives from the fact that coverage by rawinsonde observations is quite limited. Fewer than 20 regular rawinsonde stations were in operation south of 60°S during the study period; most of these were along the coast of Antarctica. However, rawinsonde observations were usually made once a day at SPO; less frequently, observations were made 2× per day. Satellite coverage and some aircraft observations have supplemented the other meteorological data available as input data to ECMWF's general circulation model. Because the gridded wind components for the pole were archived incorrectly, an average of the ECMWF winds stored at 87.5°S was used instead. This method of obtaining winds at the pole probably added to the interpolation errors intrinsic to the trajectory calculation. Kahl et al. (1989) estimated the uncertainty in trajectories produced for the Arctic, a similar data-sparse region, to be 800–1000 km after 5 days. They found that model

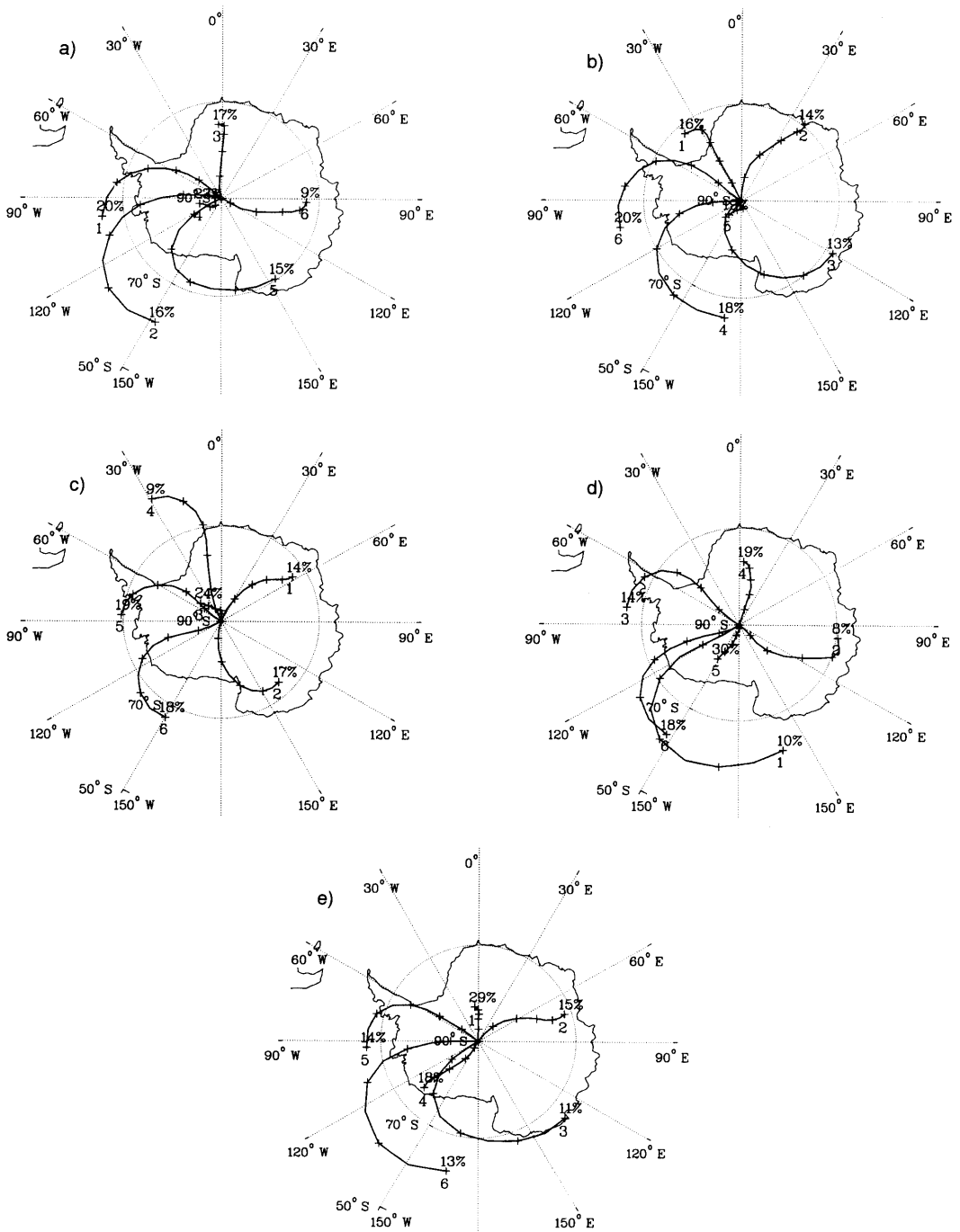

Fig. 2. Yearly atmospheric flow patterns for SPO depicted by cluster-mean back trajectories at 500 hPa for (a) 1985, (b) 1986, (c) 1987, (d) 1988, and (e) 1989. Each panel contains mean 5-day trajectories for each of six clusters. Plus signs indicate 1-day upwind intervals. The numbers 5 days upwind of SPO show (top) the percentage of trajectories occurring in that cluster and (bottom) the arbitrary cluster number used for identification.

sensitivity to the meteorological data from which trajectories are calculated can be greater than sensitivity to differences in parameterizations of vertical motion. In all likelihood, the magnitude of trajectory errors in Antarctica is similar to the estimates of Kahl et al. (1989). Such errors still allow the diagnosis of regional scale 5-day transport. Some random trajectory errors probably average out where large numbers of trajectories are summarized over years and seasons, as in the present study. However, because of interpolation errors, the uncertainty of the derived wind field, and errors introduced by the isobaric approximation, the flow patterns presented here should be viewed as rough estimates of the actual transport to SPO.

4. Cluster analysis results

Cluster-mean trajectories at the 500-hPa level were determined by year for 1985–1989. Results are shown in Fig. 2. The cluster-mean plots contain the following information: The mean trajectory for each cluster is given with plus signs indicating 1-day upwind intervals. On each cluster mean at 5 days upwind of SPO, the top number gives the percentage of all 5-day back trajectories that occur in the cluster and the bottom number identifies the cluster. The cluster identifiers (1–6) are used to distinguish one transport type from another within each plot. The numbers themselves have no inherent significance and are not related from plot to plot.

Initially we will focus on one year, 1989, to explain the graphical results of the cluster analysis. The SPO transport regimes during 1989 (Fig. 2e) include three clusters (3, 5, and 6) originating off the Antarctic coast 5 days back. These cluster means all show cyclonic curvature and arrival at SPO from the west. Cluster 6 depicts the strongest transport, originating between 60°S and 65°S. Average wind speeds in this cluster are about 10 ms^{-1} over the continent. Cluster 4, containing 18% of trajectories, depicts southwesterly flow and light winds, averaging about 4 ms^{-1}. Cluster 2 includes 15% of trajectories, those arriving from the northeast. Finally trajectories in cluster 1 occur 29% of the time; this cluster had the lightest wind speeds and mean northerly flow.

To better understand the transport patterns indicated by the cluster-mean trajectories, we plotted every trajectory in each cluster, by cluster. These "cluster-membership" plots give a qualitative feeling for the variability of the trajectories within the cluster. Fig. 3 shows membership plots for (a) cluster 2 and (b) cluster 6 determined for 1989. Only selected membership plots can be shown here because of lack of space. Although there is considerable variability within each cluster owing to natural variations of the atmosphere, the membership plots confirm that the clustering

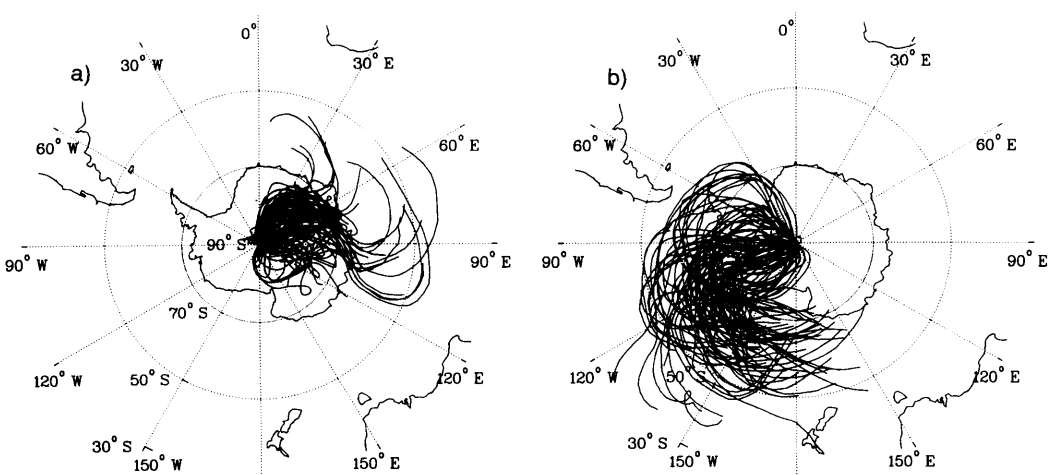

Fig. 3. Members in (a) cluster 2 and (b) cluster 6 for 1989, consisting of 5-day 500-hPa back trajectories. See Fig. 2e for the corresponding cluster means.

Tellus B/44/4-11

procedure has categorized the trajectories into six distinct groups, based on wind speed and direction along the full length of the trajectory. The cluster means are generally representative of the trajectories in the cluster, except in cases where wind speeds are very light and variable.

Trajectories were also clustered by month (5 years of Januaries, 5 years of Februaries, etc.) to show seasonal changes in flow patterns for SPO. The month-to-month changes in flow pattern are discussed in Section 5.

5. Discussion

We retain our focus on 1989 before proceeding to year-to-year and month-to-month comparisons. Cluster-membership plots for that year illustrate some noteworthy points concerning SPO flow patterns. Every 1989 transport cluster has at least some trajectories originating from the circumpolar vortex of strong westerly winds. Cluster 2 trajectories (Fig. 3a) provide evidence, based on their curvature, for the semipermanent anticyclone over northeast Antarctica. Although there are cases of long-range transport from the east, these flow patterns appear far less frequently than strong flow from the northwest to southwest. This fact attests to the asymmetry of the vortex, centered near the Ross Ice Shelf. Because of the vortex, the northern limit of transport within 5 days with few exceptions is 40°S. Clusters 3 and 5 (not shown) and cluster 6 (Fig. 3b) have numerous examples of 5-day transport from latitudes lower than 60°S, the approximate maximum sea-ice extent (Fig. 1).

Turning now to the other years, we examined the cluster means for each year for variability in SPO flow patterns from one year to the next. This variability stems mostly from the changing strength and location of storms along the Antarctic coast. For example, cluster means for 1987 (Fig. 2c) indicate that during that year, SPO experienced more vigorous northerly flow than during other years. The cluster-membership plot for cluster 4, 1987 (Fig. 4) confirms that northerly flow was very vigorous at times during 1987. Cluster means also indicated that the strength of flow from the southwest was reduced in 1987 compared with other years. This latter flow pattern, however, was exceptionally strong during 1988 (Fig. 2d). Membership for cluster 1, 1988 (Fig. 5) shows this strong southwesterly flow. These trajectories indicate that some air may have been transported from as far north as New Zealand in 5 days.

Cluster means for 3 years (1986, Fig. 2b; 1987, Fig. 2c; and 1989, Fig. 2e) indicate anticyclonic curvature in the easterly clusters accounting for 14–15% of trajectories. Easterly flow during 1985

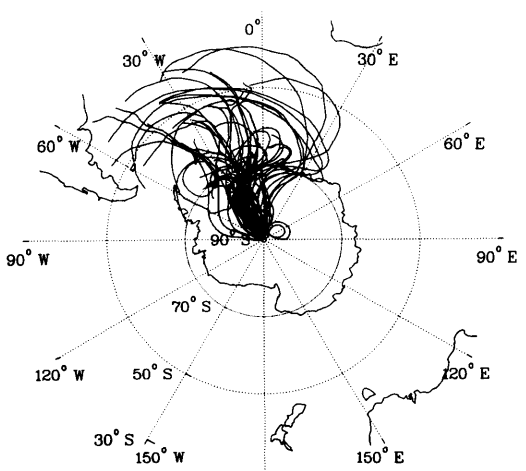

Fig. 4. Members in cluster 4, 1987, consisting of 5-day 500-hPa back trajectories. See Fig. 2c for the corresponding cluster mean. Trajectories in this plot demonstrate strong northerly flow.

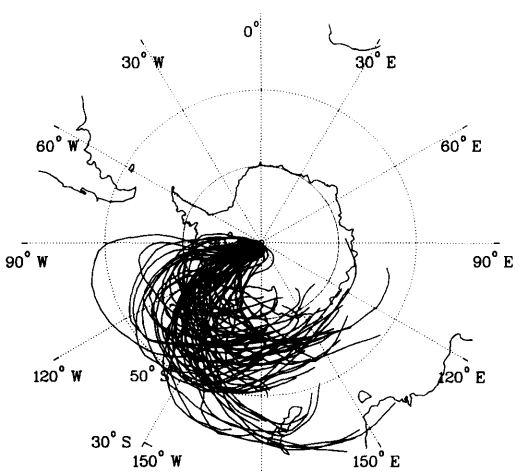

Fig. 5. Members in cluster 1, 1988, consisting of 5-day 500-hPa back trajectories. See Fig. 2d for the corresponding cluster mean. Trajectories in this plot demonstrate strong southwesterly flow.

(Fig. 2a) and 1988 (Fig. 2e) accounts for 9 and 8% of trajectories, respectively, and is weakly cyclonic in the mean. The presence of an anticyclone in the northeast quadrant of the continent would be expected to block flow from the eastern part of the vortex. This may in part account for the dearth of 5-day transport events from the eastern half of the continent. In addition, SPO is much farther from the energy-providing cyclones along the eastern coast than from those in the Ross and Weddell Seas. Long-range transport is possible from the north, as demonstrated especially in 1987. In these cases, air flows quickly poleward between a cyclone in the Weddell Sea and a ridge or anticyclone in the northeast (Stone and Kahl, 1991). The cluster means show that, in general, the strongest flow and hence the most long-range transport to SPO is from the west, accounting for 37–51% of trajectories each year. The transport clusters that describe the yearly flow patterns for SPO thus clearly reflect the asymmetry of the vortex.

The month-to-month changes in SPO flow patterns were investigated by clustering the 5 years of trajectories by month. Fig. 6 shows cluster means for three representative months. During January

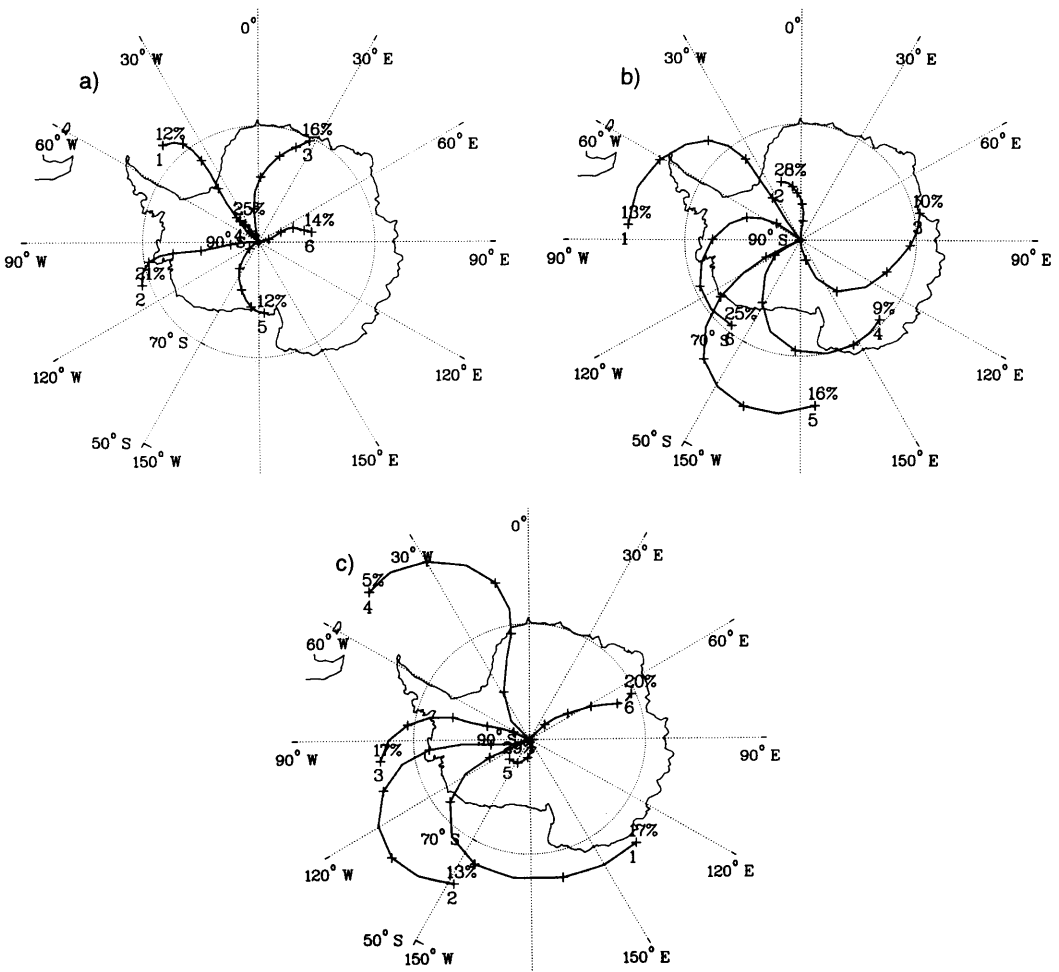

Fig. 6. Atmospheric flow patterns for SPO, for (a) January, (b) July, and (c) October, depicted by cluster-mean back trajectories at 500 hPa for the period 1985–1989. Each panel contains mean 5-day trajectories for each of six clusters. Symbols are as in Fig. 2.

(Fig. 6a) winds are lightest. Even so, it is possible that some trajectories originated over open water 5 days upwind of SPO.

Flow patterns for November, December, and February (not shown) are similar. These are transition months, still exhibiting relatively light winds; however one cluster mean, accounting for 8–13% of trajectories, originates north of 70°S 3 days upwind.

The flow patterns for March, April, May, June, and September (not shown) are stronger than those for November through February. These months all have one cluster mean showing transport from north of 70°S in 2.5 days. These strong transport clusters account for 9–18% of trajectories and arrive in the southwest quadrant, except the one for September which arrives in the northwest quadrant.

Flow patterns for July (Fig. 6b) and August (not shown) are stronger still than for the months already mentioned. July and August have two cluster means depicting transport from north of 70°S in 2.5 days. Wind speeds over the continent average about 10 ms^{-1} in these clusters which include 27–29% of trajectories during those months.

Finally, October (Fig. 4c) is the month with the strongest transport of the year. October has three cluster means originating north of 70°S 2.5 days back. The average wind speeds in these clusters are about 10–13 ms^{-1} over the continent. These clusters account for 35% of trajectories in October.

The strong transport shown during August through October occurs at an average rate of 30 times during these months, when the low-pressure center in the Ross-Amundsen-Bellingshausen Seas intensifies, bringing widespread salt storms to the interior (Murphey et al., 1991). Such storms bring increased cloudiness and aerosols to the affected regions. The intensification of these storms coincides with the equinoctial maximum in subpolar zonal winds (Schwerdtfeger, 1984).

We turn now to a comparison of isobaric versus isentropic flow as illustrated by trajectories. As an air parcel travels dry adiabatically through the atmosphere, potential temperature is conserved. Isentropic trajectories are computed along surfaces of constant potential temperature to estimate dry adiabatic vertical motions that cannot be diagnosed by isobaric trajectories. Neither the isobaric nor the isentropic model used here incorporates the moisture field or diabatic effects, such as radiational cooling and turbulent mixing, although these influences could be significant at times. Isentropic trajectories were computed to

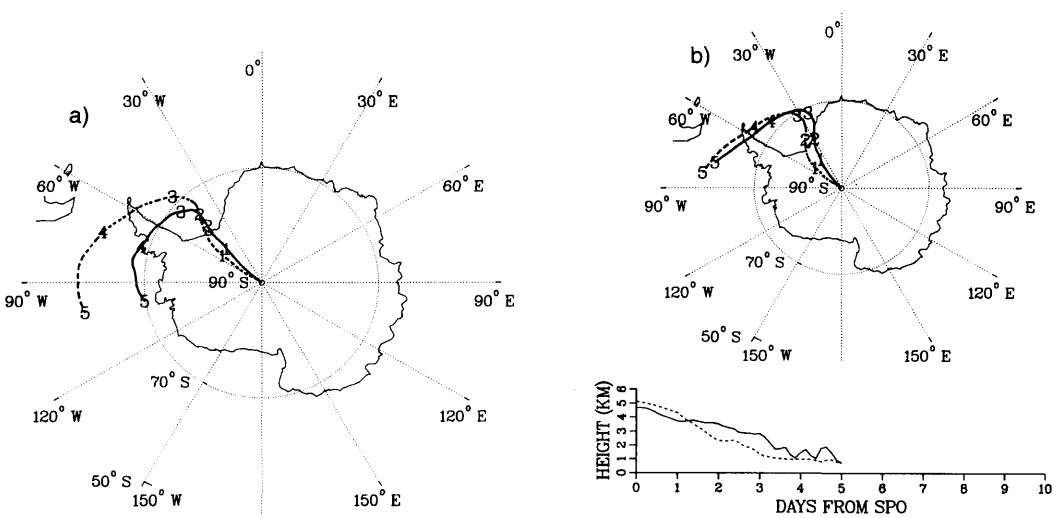

Fig. 7. (a) 500-hPa isobaric trajectories and (b) 280 K isentropic trajectories arriving at SPO on 16 July 1989. Both trajectory types are marked at 1-day upwind intervals with a numeral showing the days back. Plots below the isentropic trajectories show the heights of the trajectories. Line type distinguishes arrival time (solid = 0000 UT; dashed = 1200 UT).

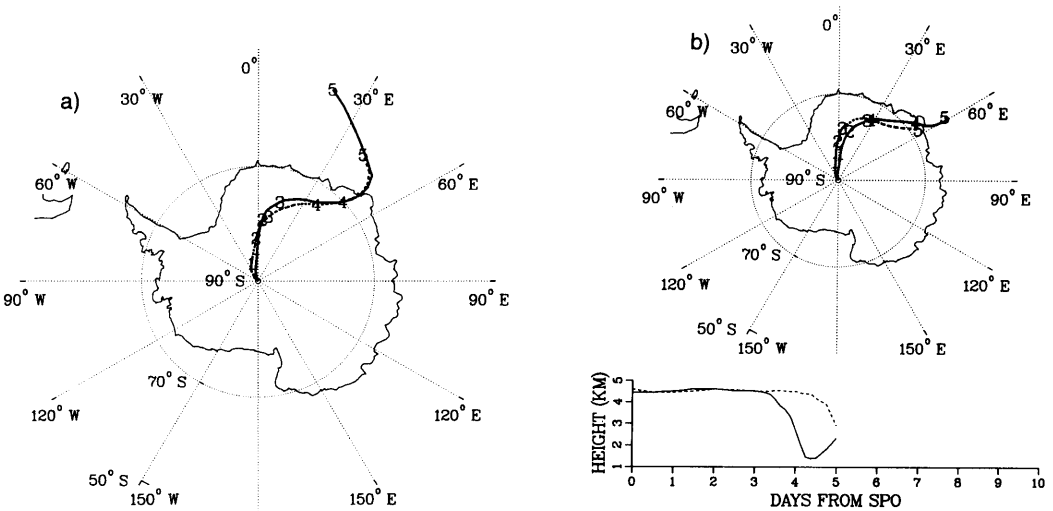

Fig. 8. (a) 500-hPa isobaric trajectories and (b) 275 K isentropic trajectories, arriving at SPO on 20 August 1989. Symbols are as in Fig. 7.

investigate how typical transport patterns change when adiabatic vertical motions are taken into account.

Figs. 7–10 present examples of isobaric trajectories compared with their isentropic counterparts. Examples were chosen from July and August, 1989, months during which rapid transport takes place. The cases shown are representative of most of the period. Both trajectory types are marked at 1-day upwind intervals with a numeral showing the days back. A solid line is used for the trajectory arriving at 0000 UT; a dashed line is used for the trajectory arriving at 1200 UT. Below the isentropic trajectories are plots showing the heights of the air parcels. Isentropic trajectories were computed on the 275-, 280-, and 285-K surfaces. Those closest to 500 hPa over SPO were compared with the isobaric trajectories.

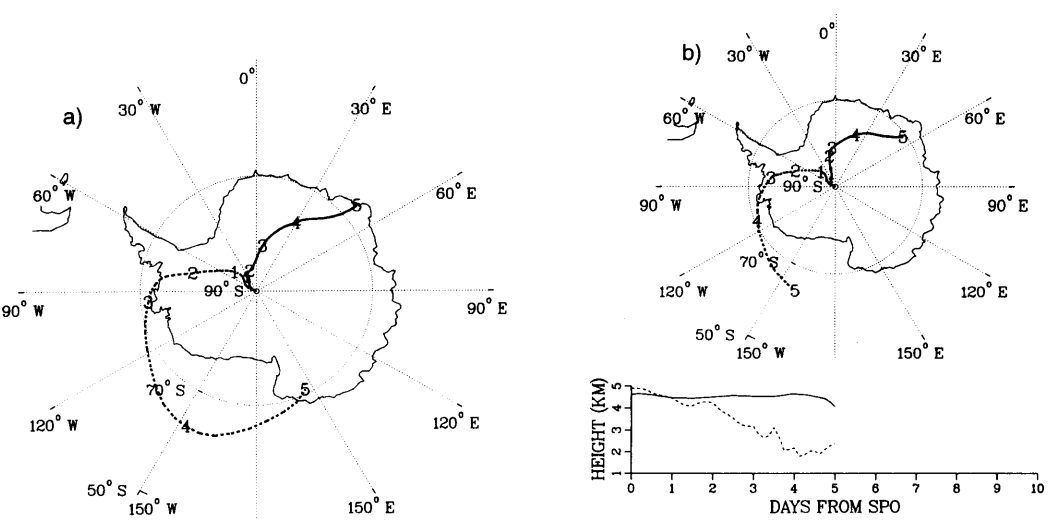

Fig. 9. As in Fig. 8, but for 21 August 1989.

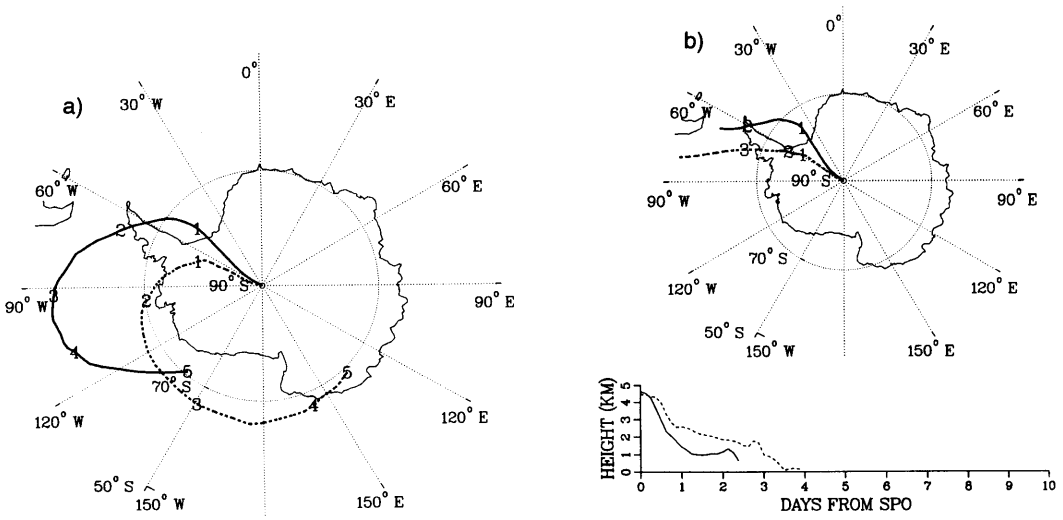

Fig. 10. As in Fig. 7, but for 13 July 1989.

First we focus on the height of the isentropic trajectories. This information sheds light on why the isobaric trajectories differ from the isentropic ones. Fig. 7 shows examples of flow from the northwest. The height plots in Fig. 7b show that, according to the isentropic model, the air parcels ascended from roughly 1 km to 5 km as they approached SPO. Fig. 8 shows flow from the northeast quadrant. Note that the height of the air parcel remains fairly constant over the continent. The height plot in Fig. 9b reiterates the pattern of ascent over west Antarctica, and steady heights over northeast Antarctica. The main reason that this pattern is revealed by the isentropic trajectories is that, on average, air is colder over the plateau east of SPO than over west Antarctica. The mean 500-hPa isotherms, though nearly circular, are offset to the east of the pole by about 8° of latitude (Schwerdtfeger, 1970). This asymmetry of the isotherms with respect to SPO stems in part from topography. The 500-hPa isotherms may be largely controlled by the elevation of the ice sheet and the extent of the radiation temperature inversion. In addition, SPO is much nearer to comparatively warm open water to the west than to the east. The result is that air parcels approaching SPO from the west cross larger temperature gradients than those from the east. The positive vertical motion seen in isentropic trajectories from the west is consistent with the fact that isentropes slope upward toward cold air (Carlson, 1981; Harris and Bodhaine, 1983).

Kutzbach and Schwerdtfeger (1967) note two other factors determining air parcel height over Antarctica: (1) cyclonic disturbances approaching the continent from the west-northwest exhibit prevailing upward vertical motion and warm-air advection, and (2) boundary layer outflow causes subsidence over east Antarctica.

Danielson (1961) described the systematic error in isobaric trajectories caused by warm-air advection associated with rising motion and (in the southern hemisphere) counterclockwise turning of the wind with height. The expected result over western Antarctica is more cyclonic curvature and higher wind speeds in the 500-hPa isobaric flow patterns, especially beyond the coast. This error is evident in Figs. 7 and 9, and is extreme in Fig. 10.

Over eastern Antarctica, where trajectory heights remain steady, there is good agreement between the isobaric and isentropic estimates of the path of the wind. However, where long trajectories originate to the east beyond the coast, the large temperature gradient experienced by the air parcel will lead to systematic errors in the isobaric estimate.

The case study determined that the isobaric flow patterns are useful in these respects: (1) The

direction at which an air parcel arrives at SPO agrees with isentropic estimates. (2) Most isobaric trajectories over east Antarctica do not differ appreciably from isentropic ones because of limited vertical motion. (3) Isobaric trajectories are usually too long and exhibit too much cyclonic curvature near and beyond the coast because of failure to account for ascent of the air parcels approaching SPO. However, the speed and curvature of the isobaric flow over west Antarctica is indicative of the vigor of the storms along the coast and their ability to transport marine air to the interior of Antarctica. (4) Because of the steep ascent of the isentropic surfaces over west Antarctica caused by the strong temperature gradient, air parcels probably originate in the boundary layer over open water around the coast. Any transport from farther northward within the boundary layer cannot be diagnosed by the isentropic model, but would be slower than that depicted by the isobaric model.

We next examined SPO 500-hPa temperature data according to clusters to investigate any differences related to transport patterns. The distributions by cluster of ECMWF gridded temperatures during July for 1985–1989 are shown in Fig. 11. These may be compared with the corresponding cluster means (Fig. 6b). We chose July as a month during which there are frequent cases of rapid transport. We see that clusters 1 and 5 exhibit the highest temperature distributions and most vigorous transport from the west. The mean temperatures for these clusters (−42.1 and −42.5°C, respectively) are about 3°C higher than the means for clusters 2 and 3. The latter clusters incorporate trajectories originating over east Antarctica. Clusters 4 and 6 indicate less vigorous flow from the west than that shown in clusters 1 and 5. The mean temperatures for clusters 4 and 6 (−44.3 and −44.6°C, respectively) fall between the extremes. These results provide further evidence of warm-air advection under conditions of rapid transport from the west.

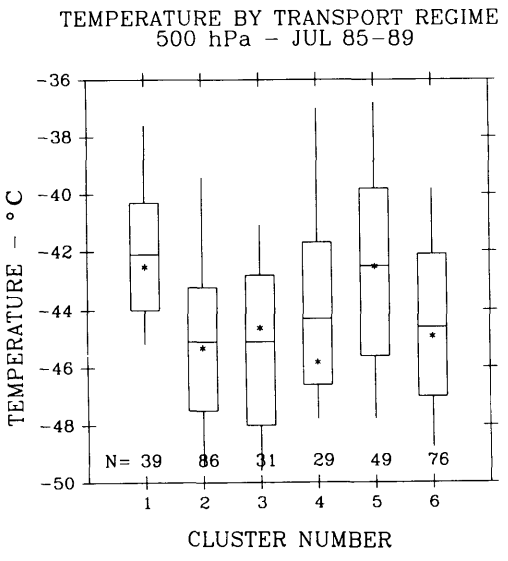

Fig. 11. Distribution of 500-hPa SPO temperatures (°C) according to transport cluster for July, 1985–1989. The asterisk is the median; the line across the box is the mean; the bottom and top of the box are the 25th and 75th percentiles; the ends of the "whiskers" are the 5th and 95th percentiles. The cluster numbers refers to flow patterns shown in Fig. 6b.

6. Conclusions

Midtropospheric flow patterns for SPO were summarized by clustering 5 years of isobaric trajectories by year and month. Isentropic trajectories for selected dates were compared to their isobaric counterparts to determine errors caused by neglecting the vertical component of the wind. SPO 500-hPa gridded temperatures were grouped by cluster to illustrate how temperatures were affected by flow regime.

Cluster means produced for each year indicated that easterly flow occurred 8–18% of the time. Flow from the east was most often anticyclonic, but sometimes weakly cyclonic. Winds were usually light enough that flow originated on the continent 5 days back. Isentropic trajectories showed little vertical motion and good agreement with isobaric counterparts.

Westerly flow patterns were the strongest and most frequent (37–51% occurrence). They were also consistently cyclonic, usually reflecting flow from storms in the Ross Sea area, the average center of the circumpolar vortex. Sample isentropic trajectories consistently indicated positive vertical motion of air parcels approaching SPO from the west, from the marine boundary layer

along the coast, to about 5 km above the pole. The effects of rapid warm-air advection caused the isobaric estimates from the west to be too fast, especially near and beyond the coast. In addition, they overestimated the cyclonic curvature in the flow.

Strong northerly flow occurred more often in some years than in others. For example cluster means show that 1987 had more vigorous northerly transport than other years, particularly 1989. Year-to-year variability was also apparent in other flow patterns. For example, the strength of southwesterly flow was reduced in 1987, and enhanced in 1988, compared with other years.

The cluster means determined for each month indicated the lightest winds of the year during January, the strongest during October. Minimal long-range transport occurred within 5 days during November, December, and February. During April through September cluster means showed strong transport 9–29 % of the time.

An analysis of gridded 500-hPa temperatures over SPO showed a marked difference in temperature distribution based on strong westerly transport versus lighter easterly flow. Vigorous westerly flow corresponded to temperatures about 3°C higher in the mean compared with temperatures during easterly flow. This result is consistent with warm-air advection from the west.

The isobaric analysis determined SPO flow patterns based on 500-hPa wind data produced by ECMWF. The isentropic case study provided information to qualitatively refine these flow patterns by determining what conditions produce errors in the isobaric trajectories. This process leads to the conclusion that the source of aerosols, heat, and moisture that is episodically transported to SPO within 5 days is usually the marine boundary layer over open waters off the west coast of Antarctica. Transport from the Weddell Sea area is also possible, but occurs less frequently. The most vigorous transport occurs in 2 to 4 days, during July through October. Preferred transport with warm-air advection from the west reflects the fact that the circumpolar vortex is asymmetric, the average isotherms are offset to the east of the pole, and the continent itself is not symmetric in shape or elevation with respect to the pole.

REFERENCES

Bodhaine, B. A., DeLuisi, J. J., Harris, J. M., Houmere, P. and Bauman, S. 1986. Aerosol measurements at the South Pole. *Tellus 38B*, 223–235.

Carlson, T. N. 1981. Speculations on the movement of polluted air to the Arctic. *Atmos. Environ. 15*, 1473–1477.

Danielson, E. F. 1961. Trajectories: Isobaric, isentropic and actual. *J. Meteorol. 18*, 479–486.

Dutton, E. G., Stone, R. S., Nelson, D. W. and Mendonca, B. G. 1991. Recent interannual variations in solar radiation, cloudiness, and surface temperature at the South Pole. *J. Clim. 4*, 848–857.

Harris, J. M. 1982. *The GMCC Atmospheric Trajectory Program.* NOAA Tech. Memo. ERL-ARL-116, NOAA Environmental Research Laboratories, Boulder, CO, 30 pp.

Harris, J. M. and Bodhaine, B. A. (Eds.) 1983. *Geophysical monitoring for climatic change*, no. 11: Summary Report 1982. NOAA Environmental Research Laboratories, Boulder, CO., 67–75.

Harris, J. M. and Kahl, J. D. 1990. A descriptive atmospheric transport climatology for the Mauna Loa Observatory, using clustered trajectories. *J. Geophys. Res. 95*, 13651–13667.

Harris, J. M., Tans, P. P., Dlugokencky, Masarie, K. A., Lang, P. M., Whittlestone, S. and Steele, L. P. 1992. Variations in atmospheric methane at Mauna Loa Observatory related to long-range transport. *J. Geophys. Res. 91*, 6003–6010.

Hogan, A. W. and Barnard, S. 1978. Seasonal and frontal variation in Antarctic aerosol concentrations. *J. Appl. Meteorol. 17*, 1458–1465.

Kahl, J. D., Harris, J. M., Herbert, G. A. and Olson, M. P. 1989. Intercomparison of three long-range trajectory models applied to Arctic haze. *Tellus 41B*, 524–536.

Kutzbach, G. and Schwerdtfeger, W. 1967. Temperature variations and vertical motion in the free atmosphere over Antarctica in the winter. *Proc. Symp. on Polar Meteorology*, Geneva 1966. WMO Tech. Note No. 87, World Meteorological Organization, Geneva, 225–248.

Moody, J. L. 1986. The influence of meteorology on precipitation chemistry at selected sites in the Eastern United States. Ph.D. thesis, University of Michigan, Ann Arbor, 176 pp.

Moody, J. L. and Galloway, J. N. 1988. Quantifying the relationship between atmospheric transport and the chemical composition of precipitation on Bermuda. *Tellus 40B*, 463–479.

Murphey, B. B., Hare, T., Hogan, A. W., Lieser, K., Toman, J. and Woodgates, T. 1991. Vernal atmo-

spheric mixing in the Antarctic. *J. Appl. Meteorol. 30*, 494–507.

Parungo, F., Bodhaine, B. and Bortniak, J. 1981. Seasonal variation in Antarctic aerosol. *J. Aerosol Sci. 12*, 491–504.

Samson, J. A. 1983. *Some characteristics of the south polar atmosphere.* MS thesis, Atmospheric Sciences Research Center Publication No. 90, State University of New York at Albany, 206 pp.

Schnell, R. C., Liu, S. C., Oltmans, S. J., Stone, R. S., Hofmann, D. J., Dutton, E. G., Deshler, T., Sturges, W. T., Harder, J. W., Sewell, S. D., Trainer, M. and Harris, J. M. 1991. Decrease of summer tropospheric ozone concentrations in Antarctica. *Nature 351*, 726–729.

Schwerdtfeger, W. 1970. The climate of Antarctica. In: *World Survey of Climatology* Vol. 14 (ed. S. Orvig). New York: Elsevier, 253–355.

Schwerdtfeger, W. 1984. Weather and climate of the Antarctic. In: *Developments in Atmospheric Science*, 15. New York: Elsevier, 261 pp.

Stone, R. S. and Kahl, J. D. 1991. Variations in boundary layer properties associated with clouds and transient weather disturbances at the South Pole during winter. *J. Geophys. Res. 96*, 5137–5144.

Trenberth, K. E. and Olson, J. G. 1988. An evaluation and intercomparison of global analyses from the National Meteorological Center and the European Centre for Medium Range Weather Forecasts. *Bull. Amer. Meteorol. Soc. 69*, 1047–1057.